

Characterization and control of phase fluctuations in elongated Bose-Einstein condensates

H. Kreutzmann¹, A. Sanpera¹, L. Santos¹, M. Lewenstein¹
 D. Hellweg², L. Cacciapuoti², M. Kottke², T. Schulte², K. Sengstock³, J. J. Arlt², and W. Ertmer²

¹ Institut für Theoretische Physik, Universität Hannover, Appelstraße 2, 30167 Hannover, Germany

² Institut für Quantenoptik, Universität Hannover, Welfengarten 1, 30167 Hannover, Germany

³ Institut für Laserphysik, Universität Hamburg, Jungiusstraße 9, 20355 Hamburg, Germany

Received: date / Revised version: date

Abstract Quasi one dimensional Bose-Einstein condensates (BECs) in elongated traps exhibit significant phase fluctuations even at very low temperatures. We present recent experimental results on the dynamic transformation of phase fluctuations into density modulations during time-of-flight and show the excellent quantitative agreement with the theoretical prediction. In addition we confirm that under our experimental conditions, in the magnetic trap density modulations are strongly suppressed even when the phase fluctuates. The paper also discusses our theoretical results on control of the condensate phase by employing a time-dependent perturbation. Our results set important limitations on future applications of BEC in precision atom interferometry and atom optics, but at the same time suggest pathways to overcome these limitations.

PACS: 03.75.Fi, 32.80.Pj, 05.30.Jp

1 Introduction

Since the first experimental observation of Bose-Einstein condensates [1] a considerable effort has been devoted to studies of low dimensional ultra-cold trapped gases [2]. There are several fundamental reasons for the interest in these systems. Firstly, atom-atom interactions can be modified in low dimensions [3]. Secondly, the physics in low dimensional systems can be remarkably different from the situation in three dimensions. For example, a one dimensional condensate in the limit of ultra-low densities should behave as a strongly correlated system of impenetrable bosons, the so-called Tonks gas [4]. The third, and perhaps the most important reason to study low temperature 1D condensates, is the particular potential that such condensates offer for applications. Proposals of atom optics and precision atom interferometry with coherent matter waves rely on placing the condensate in a 1D waveguide. Such a waveguide can be formed

in appropriately designed traps [5] or on the surface of an atom chip [6, 7]. One could then use the BEC on such a chip to perform beam splitting and, finally, beam recombination in a waveguide.

However, it has been shown that BEC in quasi 1D geometries exhibit significant phase fluctuations [8, 9]. Even at very low temperatures (of the order of fractions of the critical temperature T_c) the coherence length of such a phase-fluctuating BEC may be shorter than the size of the condensate. The condensate then exhibits a spatially varying phase pattern and is commonly called a *quasicondensate*. In the Thomas-Fermi regime [10], that is, when the nonlinear mean field energy is much larger than the kinetic energy, density fluctuations are suppressed due to their energetic cost. That is not the case, however, for the phase fluctuations. The prediction of phase fluctuations [8] was experimentally confirmed in [11, 12].

The results of our experiments set important limitations on the future applications of BEC in interferometry which employ 1D waveguides. It is, therefore, particularly important to study and characterize phase fluctuations in elongated BECs and, even more, to develop methods that allow to control the phase of these condensate.

The first part of this paper concerns the experimental investigation of two aspects of phase-fluctuating BECs. First the dynamical behavior during a time-of-flight after release from a strongly elongated trap is examined. Very good quantitative agreement between theory and experiment is established for these measurements. A second set of measurements is devoted to the investigation of the density of a phase-fluctuating trapped condensate. We confirm that the density fluctuations are strongly suppressed and show that the second order correlation function $g^{(2)}(0)$ is largely independent of the amount of phase fluctuation in our experimental regime.

The second part of the paper deals with theoretical approaches to overcome the effects of phase fluctuations.

We propose to use the technique of parametric resonance to control the overall phase of the condensate. It should be noted that parametric resonance has already been discussed in the context of BEC [13,14,15], but those studies were aimed at employing the parametric resonance to create patterns and textures in the density of trapped BECs. Clearly, for the reasons mentioned above, such a goal is not easily accomplished in highly nonlinear systems for which fluctuations of the mean field energy are costly. We, however, aim at controlling the phase of a quasi 1D condensate by applying the standard technique of modulating the trap frequency [16]. Thus, rather than to excite density modulations of the condensate, we intend to engineer its phase, such that some modes contributing to the phase fluctuations can be suppressed or enhanced without destroying the condensate.

The paper is organized as follows: In Section 2 we briefly review the physics of phase fluctuations in elongated traps, and recall the expressions describing the transformation of phase fluctuations into density modulations [11]. In Section 3 we present recent experimental results which expand the observations reported in our earlier work. These results show that a full quantitative characterization of phase fluctuations can be achieved and that density modulations are suppressed even when phase fluctuations are present in a trapped condensate. In Section 4, we describe the method of employing parametric resonance to enhance or suppress selected modes of the phase fluctuations. We present model calculations based on numerical solutions of the 1D Gross-Pitaevskii (GP) equation which governs the dynamics of the condensate.

2 Description of the phase fluctuations

For BECs in 3D trapping geometries the fluctuations of density and phase are only important in a narrow temperature range near the BEC transition temperature T_C (critical fluctuations). Outside this region, the fluctuations are suppressed and the condensate is phase and density coherent. In reduced dimensions, the situation can be rather different (see [8,17] and refs. therein): the axial phase fluctuations can manifest themselves even at temperatures far below T_C .

In the following we consider a cylindrically symmetric condensate in the Thomas-Fermi regime, where the mean field (repulsive) interparticle interaction greatly exceeds the radial ($\hbar\omega_\rho$) and axial ($\hbar\omega_x$) trap energies. At $T = 0$ its density profile has the well-known shape $n_0(\rho, x) = n_{0m}(1 - \rho^2/R_{TF}^2 - x^2/L_{TF}^2)$, where $n_{0m} = \mu/g$ is the maximum condensate density, μ is the chemical potential, $g = 4\pi\hbar^2 a/m$ is the interaction coupling constant, m is the atomic mass, and $a > 0$ the scattering length. Under the condition $\omega_\rho \gg \omega_x$, the radial size of the condensate, given by the Thomas-Fermi radius $R_{TF} = (2\mu/m\omega_\rho^2)^{1/2}$, is much smaller than the axial

size, given by the corresponding Thomas-Fermi length $L_{TF} = (2\mu/m\omega_x^2)^{1/2}$.

The phase fluctuations can be described by solving the Bogoliubov-de Gennes equations describing elementary excitations of the condensate. The quantum field annihilation operator of atoms can be written as $\hat{\psi}(\mathbf{r}) = \sqrt{n_0(\mathbf{r})} \exp(i\hat{\phi}(\mathbf{r}))$, where $\hat{\phi}(\mathbf{r})$ is the operator of the phase, and the density fluctuations have already been neglected following the arguments discussed above. The single-particle correlation function is then expressed through the mean square fluctuations of the phase (see e.g. [18]):

$$\langle \hat{\psi}^\dagger(\mathbf{r}) \hat{\psi}(\mathbf{r}') \rangle = \sqrt{n_0(\mathbf{r})n_0(\mathbf{r}')} \exp\{-\langle [\delta\hat{\phi}(\mathbf{r}, \mathbf{r}')]^2 \rangle / 2\}, \quad (1)$$

with $\delta\hat{\phi}(\mathbf{r}, \mathbf{r}') = \hat{\phi}(\mathbf{r}) - \hat{\phi}(\mathbf{r}')$. The operator $\hat{\phi}(\mathbf{r})$ is given by (see e.g. [19])

$$\hat{\phi}(\mathbf{r}) = [4n_0(\mathbf{r})]^{-1/2} \sum_j f_j^+(\mathbf{r}) \hat{a}_j + \text{h.c.}, \quad (2)$$

where \hat{a}_j is the annihilation operator of the excitation with quantum number j and energy ϵ_j , $f_j^+ = u_j + v_j$, and the excitation functions u_j, v_j are determined by the Bogoliubov-de Gennes equations in the Thomas-Fermi limit.

The “low-energy” axial excitations (with energies $\epsilon_j < \hbar\omega_\rho$) have wavelengths larger than R_{TF} and exhibit a pronounced 1D behavior. Hence, one expects that these excitations give the most important contribution to the long-wave axial fluctuations of the phase. The solution of the hydrodynamic counterpart of the Bogoliubov-de Gennes equations in the Thomas-Fermi limit for such low-energy axial modes yields the spectrum $\epsilon_j = \hbar\omega_x \sqrt{j(j+3)/4}$ [20], where j is a positive integer. The wavefunctions f_j^+ of these modes have the form

$$f_j^+(\mathbf{r}) = \sqrt{\frac{(j+2)(2j+3)gn_0(\mathbf{r})}{4\pi(j+1)R_{TF}^2 L_{TF} \epsilon_j}} P_j^{(1,1)}\left(\frac{x}{L_{TF}}\right), \quad (3)$$

where $P_j^{(1,1)}$ are Jacobi polynomials. Note that the specific form of the excitation spectrum and the x -dependence of the mode functions results in the quasi 1D limit from the integration of the mode functions over the transverse directions, as pointed out for instance in Ref. [20].

The thermal fluctuations of the phase behave for distances shorter than $\simeq 0.4 L_{TF}$ as:

$$\langle [\delta\hat{\phi}(x, x')]^2 \rangle_T = \delta_L^2 |x - x'| / L_{TF}, \quad (4)$$

where δ_L^2 is a measure for the amount of phase fluctuations present in the condensate and given by [9]

$$\delta_L^2(T) = T/T_\phi = 32\mu k_B T / 15N_0(\hbar\omega_x)^2, \quad (5)$$

where k_B is the Boltzmann constant and $l_\phi = L_{TF}/\delta_L^2$ can be interpreted as a phase coherence length. Substituting the chemical potential in the Thomas-Fermi

regime in Eq. (5), one obtains the direct dependence on the experimental parameters:

$$L_{\text{TF}}/l_\phi = 16 \left(\frac{am^{1/2}}{15^{3/2}\hbar^3} \right)^{2/5} \frac{k_B T}{N_0^{3/5}} \left(\frac{\lambda}{\omega_x} \right)^{4/5}. \quad (6)$$

Strong phase fluctuations are thus associated with high trap aspect ratios $\lambda = \omega_\rho/\omega_x$, weak axial confinement ω_x , high temperatures T and small numbers of condensed atom N_0 .

The signature of a fluctuating phase can be observed experimentally as density modulations (stripes) in the ballistic expansion. The formation of these stripes can be understood as follows: After switching off the trap, the mean field interaction rapidly decreases and the axial phase pattern is converted into a velocity distribution. This spatial velocity distribution leads to the appearance of stripes in the density after a time-of-flight. These stripes have been described analytically [12] using a generalization of the Bogoliubov-de Gennes equation for the self-similar solution (see e.g. [10, 21, 22]). This equation describes the ballistic expansion in presence of fluctuations. By denoting the density as $n_0 + \delta n$ and the phase as $\phi_0 + \phi$ we obtain the analytic expression for the relative density fluctuations

$$\frac{\delta \hat{n}}{n_0} = 2 \sum_j \tau^{-(\epsilon_j/\hbar\omega_\rho)^2} \sin \left[\frac{\epsilon_j^2 \tau}{\mu \hbar \omega_\rho (1 - (x/L_{\text{TF}})^2)} \right] \hat{\phi}_j, \quad (7)$$

where the sum extends over the axial modes, $\tau = \omega_\rho t$, t is the time-of-flight and $\hat{\phi}_j$ is the contribution of the j -th mode to the phase operator in Eq. (2).

By taking the thermal average of the square of Eq. (7) [12], one obtains a closed relation for the mean square density fluctuations [23]

$$\left\langle \left(\frac{\delta n(x, t)}{n_0(x)} \right)^2 \right\rangle = \frac{T}{T_\phi} C^2(N_0, \omega_\rho, \omega_x, x, t), \quad (8)$$

where

$$\begin{aligned} C^2(N_0, \omega_\rho, \omega_x, x, t) = & \frac{1}{2} \sum_{j=1}^{\infty} \sin^2 \left(\frac{(j+3/2)^2}{4\alpha(1 - (x/L_{\text{TF}})^2)} \right) e^{-\left(\frac{\omega_x}{\omega_\rho}\right)^2 \frac{(j+3/2)^2}{2} \ln(2\omega_\rho t)} \times \\ & \left(\frac{(j+2)(2j+3)}{j(j+1)(j+3)} \right) \left(P_j^{(1,1)} \left(\frac{x}{L_{\text{TF}}} \right) \right)^2, \end{aligned} \quad (9)$$

with $\alpha = \mu/\hbar\omega_x^2 t$.

3 Experimental Results

3.1 Experimental setup

The experimental setup used to observe phase-fluctuating Bose-Einstein condensates has been described elsewhere [11, 12]. Here we emphasize the main features of

the apparatus and the technical changes that have led to the observation of more pronounced effects of phase fluctuations in the ballistic expansion of an elongated condensate.

We have adapted the trap geometry to obtain aspect ratios $\lambda > 100$ and reduced axial confinement. These high trap aspect ratios are achieved by axial decompression of our cloverleaf trap [24], lowering the currents in both the pinch coils and their bias coils.

For the experiments reported here, a Bose-Einstein condensate of ^{87}Rb atoms in the $|F=1, m_F=-1\rangle$ state is produced in the axially decompressed trap with axial and radial trapping frequencies 3.4 Hz and 380 Hz respectively, by using the following procedure. We load a magneto-optical trap with a few times 10^8 atoms from a chirp slowed thermal beam, followed by a short period of sub-Doppler cooling. Part of the sub-Doppler cooling stage operates without repumping the atoms from the $|F=1\rangle$ state, letting them accumulate in the lower hyperfine state. After optical pumping to the low field seeking $m_F=-1$ state, the atomic cloud is loaded into a cloverleaf magnetic trap. A cleaning light pulse on resonance with the $|F=2\rangle \rightarrow |F'=2\rangle$ transition then removes all remaining $|F=2\rangle$ atoms from the trap. Finally, the atomic cloud is adiabatically compressed to allow efficient radio frequency evaporative cooling. The condensate is loaded in the axially decompressed trap by using a two step evaporation procedure. The initial evaporative cooling is performed in our standard trap with aspect ratio 26, then the trap is ramped to the high aspect ratio configuration, and the final evaporation is carried out in that trapping geometry. After waiting for 4 seconds to allow the system to reach an equilibrium state we switch off the trapping potential within 200 μs and wait for a variable time-of-flight before detecting the atomic cloud by resonant absorption imaging.

The experimental observation of phase fluctuations profits from this adapted trap configuration as indicated by Eq. (6). Our present measurements show strong fluctuations both due to the high aspect ratio and the weak axial confinement of our trap. These lead to a large axial condensate size (in the elongated trap, $2L \sim 300 \mu\text{m}$) with respect to the detection resolution of $\sim 5 \mu\text{m}$, thus favoring the observation of structures in the condensate density after time-of-flight.

3.2 Expansion dynamics

Phase fluctuations transform into density modulations during ballistic expansion. It was shown that the general dependence on temperature, trapping potential and number of atoms given in Eq. (3) of [11] agrees qualitatively with the experimental observations. Most data was acquired after a long time-of-flight of 25 ms since the effect of phase fluctuations is best observed then. However, here we present observations of the dynamical

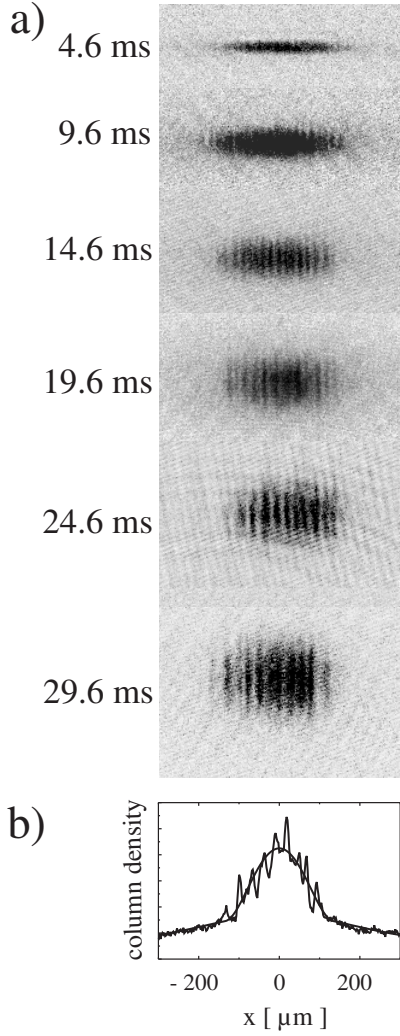


Fig. 1 (a) Absorption images of the expanded clouds after various times-of-flight. The images show $\sim 7 \times 10^4$ condensed atoms at a temperature of $\sim 0.6 T_C$. The atomic clouds are released from a magnetic trap with axial and radial frequencies of $2\pi \times 3.4$ Hz and $2\pi \times 380$ Hz respectively. Due to the destructive imaging technique, each image shows a different condensate. (b) The line density profile of the last time-of-flight image is compared with the corresponding bimodal fitting function.

transformation of phase fluctuations into density modulations and quantitatively compare them to the theoretical predictions.

Fig. 1(a) shows typical images of the ballistically expanded clouds for various times-of-flight t . The atomic samples were released from a magnetic trap with axial and radial trapping frequencies of 3.4 Hz and 380 Hz, respectively. They contain $\sim 7 \times 10^4$ condensed atoms at a temperature of $\sim 0.6 T_C$. Under these experimental conditions, the phase coherence length in units of the condensate size is $l_\phi/2L \sim 1/12$. The usual anisotropic expansion of the condensates is clearly visible. The line density profile in Fig. 1(b) shows the large influence of

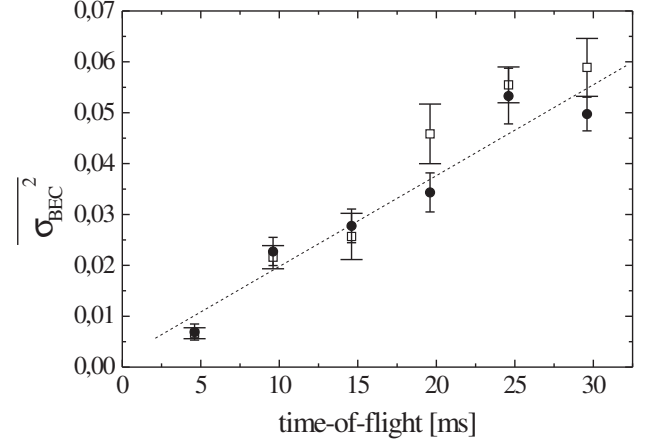


Fig. 2 Black circles: Measurements of the normalized spatial average of the phase fluctuations σ_{BEC}^2 as a function of the time-of-flight. Each data point is the average of 15 measurements. Open squares: Theoretically predicted values. Line: Fit to the measured data as a guide to the eye. The error bars indicate the statistical error.

phase fluctuations on the expansion of the condensate. To avoid high optical densities, which would influence the visibility of density modulations, we detuned the detection laser with respect to the atomic resonance for short times-of-flight.

The amount of phase fluctuations present in a given BEC was determined by comparing the observed line density profile with the expected bimodal profile when no phase fluctuations are present. In this bimodal profile the BEC fraction is described by a parabolic Thomas-Fermi component and the thermal cloud by a Gaussian distribution, both integrated along the radial direction. The deviation of the experimental density profile from the fitted function is calculated at every data point in the interval $-0.5 < x/L < 0.5$ and normalized by the fitted condensate density at that point. The average of the squares of these values is called σ_{BEC}^2 and represents a normalized spatial average of the phase fluctuations in a single condensate. The temperature and particle number of each condensate were determined by separate 2D fits to the absorption images.

Note that phase fluctuations in an elongated BEC are stochastic. During the expansion, the instantaneous phase of the BEC at the time of release is converted into density modulations and therefore images taken under the same initial conditions can look significantly different. Indeed, we observe a large spread of our experimental data and, therefore, each data point in Fig. 2 represents the average of 15 measurements.

Fig. 2 shows the observed density modulations (black circles) as a function of the free expansion time. All images were taken under the conditions given in Fig. 1. The data clearly shows how the effect of phase fluctuations on the expansion dynamics increases with the time-of-flight.

To compare our measurements with theory, each experimental realization (each condensate) was modeled individually as explained below and for each time-of-flight the average of all experimental realizations is compared to the average of all modeled realizations. Using the experimentally determined temperature and atom number, the expectation value of the density modulations for each realization was calculated according to Eq. (8). Analogous to the experimental procedure, a normalized spatial average over the range $-0.5 < x/L < 0.5$ was deduced. The theoretical prediction in Fig. 2 takes the limited resolution of our imaging system into account [12].

We obtain very good quantitative agreement between our results and the theoretical predictions, confirming that the transfer mechanism of phase fluctuations into density modulations during time-of-flight is well understood.

3.3 Suppression of density fluctuations

The theoretical description of phase fluctuations is based on the prediction [8] that density modulations are strongly suppressed in the magnetic trap. In the Thomas-Fermi regime, where the mean field energy dominates over the kinetic energy, the excitation of density modulations requires a high energetic cost on the order of the chemical potential. The measurements reported in Fig. 2 clearly show that the observed density modulations are suppressed as the time-of-flight approaches zero. However, this does not rule out the existence of density modulations on a length scale smaller than our experimental resolution.

The suppression of density fluctuations can be verified experimentally by measuring the second order correlation function $g^{(2)}(\mathbf{r}_1 - \mathbf{r}_2)$ of the field operator $\hat{\Psi}(\mathbf{r})$. In second quantization formalism,

$$g^{(2)}(\mathbf{r}_1 - \mathbf{r}_2) = \frac{\langle \hat{\Psi}^\dagger(\mathbf{r}_1) \hat{\Psi}^\dagger(\mathbf{r}_2) \hat{\Psi}(\mathbf{r}_2) \hat{\Psi}(\mathbf{r}_1) \rangle}{n(\mathbf{r}_1)n(\mathbf{r}_2)}. \quad (10)$$

In particular, $g^{(2)}(0)$ gives the correlation function of the atomic density for $\mathbf{r}_1 = \mathbf{r}_2$. As shown in [25], $g^{(2)}(0)$ is directly related to the expectation value of the interaction energy U by

$$\langle U \rangle = \frac{2\pi\hbar^2 a}{m} g^{(2)}(0) \int d^3r n^2(\mathbf{r}). \quad (11)$$

In the Thomas-Fermi regime, only the interaction energy $\langle U \rangle$ contributes to the kinetic energy of the condensate after ballistic expansion. The presence of density fluctuations would however lead to an increase of the observed release energy due to the presence of repulsive particle interactions. Hence, the ratio of the release energy and the calculated interaction energy in Thomas-Fermi approximation gives the value of $g^{(2)}(0)$. The energy due to

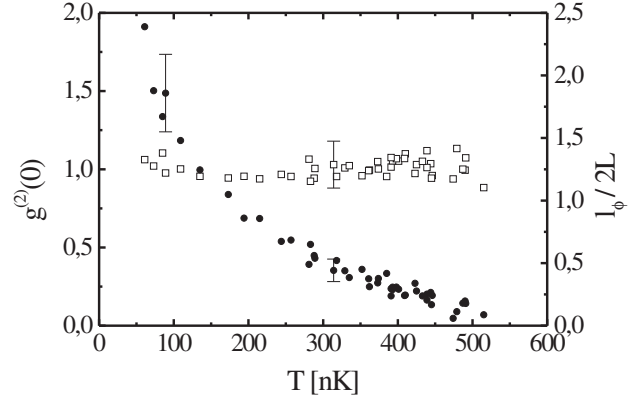


Fig. 3 Open squares: Measurements of $g^{(2)}(0)$ as a function of temperature for phase-fluctuating $|F=1\rangle$ condensates in a $\lambda = 30$ trap. Black dots: Calculated phase coherence length l_ϕ , in units of the axial condensate size $2L$, for the experimental conditions of each data point. The error bars indicate the maximum error.

phase fluctuations is small compared to the interaction energy (for typical parameters $\sim 0.5\%$) and can therefore be neglected in release energy measurements.

From earlier release-energy measurements, the product $a g^{(2)}(0)$ has been determined [26, 22, 24]. We have performed such a measurement for phase-fluctuating condensates.

Fig. 3 shows $g^{(2)}(0)$ (open squares) as a function of temperature for atoms in the $|F=1\rangle$ state in a trap with $\lambda = 30$. We use this weakly elongated trap, because this trapping geometry enables us to use the sample temperature to tune from nearly pure to strongly phase-fluctuating condensates experimentally.

The same graph also shows the calculated phase coherence length l_ϕ according to Equation (6) for the experimental conditions of each data point (black circles). As the temperature of the sample is raised, the phase coherence length decreases and becomes significantly shorter than the condensate size. Thus, our measurements clearly reach the regime of quasicondensation. However, the graph shows that the second-order correlation function is largely independent of the condensate temperature T , and that it is consistent with the expected value $g^{(2)}(0) = 1$. These measurements give an upper limit for the density modulations present in a phase-fluctuating condensate, and clearly distinguish our samples from thermal clouds where, due to bunching effects, $g^{(2)}(0) = 2$ and large density fluctuations are present on small scales.

4 Controlling the phase

Parametric resonance refers to the exponentially large response of a system of a periodic external perturbation [27] for some specific set of parameters. Although

parametric resonance is a very well established phenomenon in linear systems, it was shown in [13] that parametric resonance can also occur in Bose-Einstein condensates. Normally one aims at using parametric resonance in order to modulate the condensate density by means of a relatively small periodic perturbation. However, in the Thomas-Fermi regime, as mentioned above, modulations of the density require large energies. In this Section we suggest a way to shape the overall phase by modulating the trap with a small amplitude for a short time.

4.1 Theoretical methods

To illustrate the effect of the perturbation on the phase of a quasicondensate, we numerically solve the 1D Gross-Pitaevskii equation for different initial conditions. We assume a zero temperature BEC in the Thomas-Fermi regime containing 5×10^4 ^{87}Rb atoms trapped in a 1D confining potential with an (axial) frequency of $\omega_x = 2\pi \times 14$ Hz. The parabolic density profile is then given by $n_0(x) = n_{0\text{m}}(1 - x^2/L_{\text{TF}}^2)$ where $L_{\text{TF}} = (2\mu/m\omega_x^2)^{1/2}$ and $n_{0\text{m}} = \mu/g$. The coupling constant g in one dimension can be derived by averaging the 3D interactions over the radial density profile. We first evolve the wavefunction according to the time dependent GP equation in imaginary time to obtain the condensate wavefunction at $T = 0$. We ensure that the initial phase of the condensate is constant before imposing a fluctuating phase corresponding to a fixed temperature T on the condensate wavefunction. In strictly 1D, one expects that for temperatures $T_{\text{d}} \gg T \gg T_{\phi}$ phase fluctuations are present whereas density fluctuations are suppressed [8]. Here $k_{\text{B}}T_{\text{d}} \approx N\hbar\omega_x$ is the degeneracy temperature [28], and $T_{\phi} = T_{\text{d}}\hbar\omega_x/\mu$ is the characteristic temperature for the appearance of the phase fluctuations.

Applying the same procedures for the 1D case as described in Section 2 for the 3D case, the field annihilation operator can be written as $\hat{\psi}(x, t = 0) = \sqrt{n_0(x)} \exp(i\hat{\phi}(x))$. The operator of the phase is given by (see [8, 19])

$$\hat{\phi}(x) = \frac{1}{\sqrt{4n_0(x)}} \sum_{j=1}^{\infty} f_j^+(x) \hat{a}_j + \text{h.c.} \quad (12)$$

where, as before, \hat{a}_j is the annihilation operator of the excitation with quantum number j , $f_j^+ = u_j + v_j$ and u_j , v_j are the excitation functions determined through the Bogoliubov-de Gennes equations in the Thomas-Fermi limit. The solution of these 1D equations gives the spectrum $\epsilon_j = \hbar\omega_x \sqrt{j(j+1)/2}$ [29]. The functions f_j^+ have now the form

$$f_j^+(x) = \sqrt{\frac{(j+1/2)}{L_{\text{TF}}}} \left[\frac{2\mu}{\epsilon_j} (1 - z^2) \right] P_j(z), \quad (13)$$

where $P_j(z)$ are the Legendre polynomials and $z = x/L_{\text{TF}}$. Note, that these solutions correspond to the strictly 1D case and differ from those obtained in the quasi 1D case described by (3). The qualitative and, to great extent, quantitative character of the solutions (13) and (3) is, however, similar.

The random phase of the condensate is numerically simulated by replacing the operators \hat{a}_j and \hat{a}_j^\dagger in Eq. (12) by Gaussian random variables α_j and α_j^* , with the correlation $\langle \alpha_j^* \alpha_{j'} \rangle = \delta_{jj'} N_j$, where N_j is the occupation number for the quasiparticle mode j for a given temperature T .

Once the phase is imposed, we apply a periodic perturbation $\alpha \sin(\omega_s t)$ to the trapping potential:

$$\omega_x^2 \rightarrow \omega_x^2 (1 + \alpha \sin(\omega_s t)). \quad (14)$$

The amplitude α of the perturbation is small and ranges between 0.05 and $0.20 \ll 1$, whereas the frequency ω_s ranges from ω_x to several times ω_x . The perturbation acts for a short period of time t (the simulations were performed for 2, 6 and 12 periods of modulation $2\pi/\omega_s$). After switching off the perturbation the amplitudes of the different modes participating in the fluctuations of the phase are calculated. The thermal fluctuations of the phase for the temperature range considered here are mostly provided by the low excitation modes ($j < 50$). We calculate the amplitude of these modes as a function of the frequency of the perturbation.

4.2 Numerical results

Our calculations show that the positive and negative frequency modes couple resonantly and that by appropriately tuning the frequency of the perturbation one can selectively suppress some modes and enhance others. The enhancement, however, is not particularly strong, since we do not amplify any mode (except the second mode which arises directly due to the parametric modulation) much above its initial value provided by Eq. (13). Note that the odd modes can only be excited if the symmetry is broken, e.g. by the existence of phase fluctuations.

Figure 4 displays the amplitudes of the first two modes for different initial temperatures as a function of the frequency ω_s . The second mode, which corresponds to the density breathing mode, is strongly enhanced due to the perturbation of the trap. This mode amplitude can be calculated in the Thomas-Fermi regime by using a self similar solution of the GP equation [21, 22] describing the dynamics of the bare condensate that implies appearance of a phase quadratic in x . Indeed, only for sufficiently large temperatures ($T \sim 0.5 T_{\text{C}}$), its frequency dependence starts to deviate significantly from its behavior at $T = 0$.

To show the effect of the fluctuating phase on the final amplitudes, we subtract the phase a pure condensate would have acquired under the same perturbation

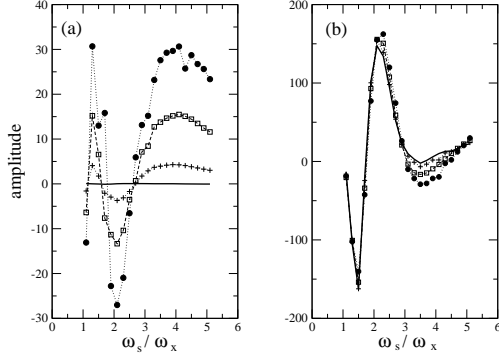


Fig. 4 (a) Amplitude of the first and (b) second mode as a function of the modulation frequency ω_s . The perturbation was applied for $t = 2 \times 2\pi/\omega_s$ with an amplitude of $\alpha = 0.05$. The solid line indicates the final amplitude starting from a pure condensate ($T = 0$); crosses correspond to a quasicondensate at initial temperature of $T = 0.01 T_C$, open squares to $T = 0.1 T_C$ and circles to $T = 0.4 T_C$. The same set of random coefficients were used in all the cases.

from our results. Figure 5 displays the modulus square of such amplitudes normalized to their initial values for the first four modes. The amplitudes of the high excited modes (app. $j > 4$) are practically equal and negligibly small compared to the lower modes therefore the lower modes dominate the dynamics of the phase. Only those modes show clear maxima and minima as a function of the modulation frequency ω_s . Resonances between different modes may appear when

$$\omega_s = |\Omega_i \pm \Omega_j|, \quad (15)$$

where $\Omega_i = \epsilon_i/\hbar$. In order to observe resonances it is necessary that the energy differences between the modes correspond to multiples of the modulation frequency, otherwise the system behaves irregularly. In the 1D case, the excitation modes are quite regularly separated by approximately $\omega_x/\sqrt{2}$ ($\approx 0.71 \omega_x$). However, in nonlinear systems, the resonance frequencies undergo shifts which can already be quite significant at small perturbations [30]. For the first mode (Fig. 5), we find clear resonances at $\omega_s/\omega_x \simeq 1.4, 2.1$ and 4.0 . One is tempted to attribute the first two resonances to the coupling with $j = 3$ and $j = 4$ mode. The second mode, which dominates the dynamics — since this mode is enhanced by the perturbation — shows three maxima at $\omega_s/\omega_x \simeq 1.4, 2.1$ and 3.6 . The analysis of maxima for the third and higher modes becomes quite complex. For the third mode, we find maxima at $\omega_s/\omega_x \simeq 1.4, 1.7, 2.4, 3.4$ and 5.0 . Starting from the fourth mode it becomes difficult to associate the maxima with specific resonances.

It is important to stress here that for the lower modes, the position of the maxima does not depend on the random generated phase. This fact clearly confirms that we are dealing here with resonances between different modes. By increasing the perturbation time the spectrum changes, as expected, since this is a time dependent

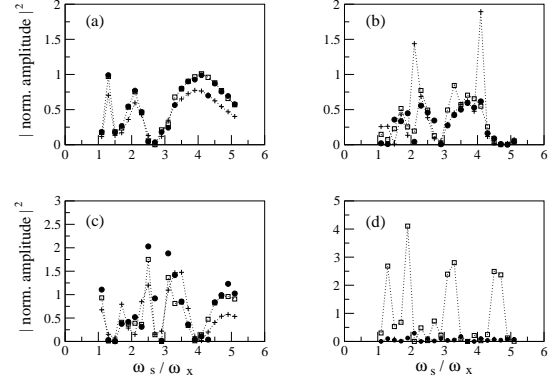


Fig. 5 Modulus square of the exciting mode amplitudes normalized to their initial value at $t = 0$. The contribution corresponding to $T = 0$ has been previously subtracted. (a) (b) (c) and (d) correspond to amplitudes of the first second, third and fourth mode for the same parameters as Fig. 4.

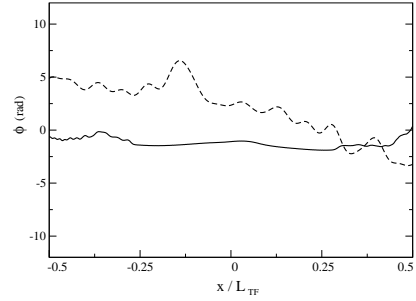


Fig. 6 The dotted line shows a typical phase pattern for $\omega_s = 2\pi \times 14$ Hz, $\lambda = 51$ and initial temperature $T = 0.4 T_C$, the solid line shows the final phase after applying the time dependent perturbation for a duration of two cycles with $\alpha = 0.05$ and $\omega_s = 5.7 \omega_x$.

effect, and more peaks appear. However with the exception of the second one, no enhancement of the modes is observed. By increasing the amplitude α of the perturbation, the second mode becomes much more enhanced, but again the amplitudes of the other modes (normalized to their initial values at $t = 0$) do not. In other words, we do not find an exponential parametric amplification by tuning the frequency to $2\Omega_i/n$ where n is a positive integer. Nevertheless, the fact that the amplitudes of the lower modes display well defined maxima and minima allows to shape the overall phase of the quasicondensate. As an example, in Fig. 6 we show the initial fluctuating phase of a quasicondensate at $T = 0.4 T_C$, and its final phase after the perturbation is switched off. In the range $|x/L_{TF}| < 0.5$ the final phase becomes practically constant demonstrating that the initial fluctuations can be significantly suppressed using the parametric modulation technique. To achieve this specific phase we chose the frequency ω_s such that the lower modes have approximately the same amplitude value.

5 Conclusion and outlook

In this paper we analyze fluctuations of the phase of quasi 1D condensates at temperatures of the order of fractions of T_C . The dynamical transformation of phase fluctuations into density modulations was observed as function of free expansion time. A detailed comparison of the statistical average of the modulation with the theoretical prediction shows excellent agreement. It was also verified experimentally that density modulations of a phase fluctuating BEC in the trap are strongly suppressed. The quantitative understanding of the transfer of phase fluctuations into density modulations opens a pathway to use phase fluctuations for condensate thermometry.

Phase fluctuations impose restrictions on the applicability of quasi 1D condensates in atom optics and precision atom interferometry. We show that a possible mechanism to control the overall phase of a quasi 1D condensate is to use a small periodic perturbation of the trap. In this way, only few of the modes responsible for the phase fluctuations become relevant. Furthermore, by properly tuning the frequency, time and amplitude of the external perturbation one can resonantly couple the different relevant low order modes, so that some of them are enhanced and others are inhibited. This method suggest a pathway to control phase fluctuations and overcome their undesired effects.

We acknowledge valuable discussions with G. Shlyapnikov, D. S. Petrov and C. Bordé. This work is supported by the *Deutsche Forschungsgemeinschaft* within the SFB 407 and the Schwerpunktprogramm "Wechselwirkungen ultrakalter atomarer und molekularer Gase", Alexander von Humboldt Stiftung, and the European Science Foundation (ESF) within the BEC2000+ programme.

References

1. M. H. Anderson, J. R. Ensher, M. R. Matthews, C. E. Wieman, and E. A. Cornell, *Science* **269**, 198 (1995); K. B. Davis, M.-O. Mewes, M. R. Andrews, N. J. van Druten, D. S. Durfee, D. M. Kurn, and W. Ketterle, *Phys. Rev. Lett.* **75**, 3969 (1995); C. C. Bradley, C. A. Sackett, and R. G. Hulet, *Phys. Rev. Lett.* **78**, 985 (1997); D. Fried, T. C. Killian, L. Willmann, D. Landhuis, S. C. Moss, D. Kleppner, and T. J. Greytak, *Phys. Rev. Lett.* **81**, 3811 (1998).
2. A. Görlitz, J. M. Vogels, A. E. Leanhardt, C. Raman, T. L. Gustavson, J. R. Abo-Shaeer, A. P. Chikkatur, S. Gupta, S. Inouye, T. Rosenband, and W. Ketterle, *Phys. Rev. Lett.* **87**, 130402 (2001); A. I. Safonov, S. A. Vasilyev, I. S. Yasnikov, I. I. Lukashevich, and S. Jaakkola, *Phys. Rev. Lett.* **81**, 4545 (1998); M. Greiner, I. Bloch, O. Mandel, T. W. Hänsch, and T. Esslinger, *Phys. Rev. Lett.* **87**, 160405 (2001); I. Bouchoule, M. Morinaga, C. Salomon, and D. S. Petrov, *Phys. Rev. A* **65**, 033402 (2002); S. Burger, F. S. Cataliotti, C. Fort, P. Maddaloni, F. Minardi, and M. Inguscio, *Eur. Phys. Lett.* **57**, 1 (2002).
3. M. Olshanii, *Phys. Rev. Lett.* **81**, 938 (1998); G. V. Shlyapnikov, *Comptes rendus de l'Académie des sciences - Série IV - Physique - Astrophysique* **2**, 407 (2001); see also [8] and [17].
4. L. Tonks, *Phys. Rev.* **50**, 955 (1936); M. Girardeau, *J. Math. Phys.* **1**, 516 (1960); M. Girardeau and E. M. Wright, *Laser Phys.* **12**, 8 (2002).
5. K. Bongs, S. Burger, S. Dettmer, D. Hellweg, J. Arlt, W. Ertmer, and K. Sengstock, *Phys. Rev. A* **63**, 031602 (2001).
6. J. Denschlag, D. Cassettari, and J. Schmiedmayer, *Phys. Rev. Lett.* **82**, 2014 (1999); J. Reichel, W. Hänsel, and T. W. Hänsch, *Phys. Rev. Lett.* **83**, 3398 (1999); D. Müller, D. Z. Anderson, R. J. Grow, P. D. D. Schwindt, and E. A. Cornell, *Phys. Rev. Lett.* **83**, 5194 (1999).
7. W. Hänsel, P. Hommelhoff, T. W. Hänsch, and J. Reichel, *Nature* **413**, 498 (2001); H. Ott, J. Fortagh, G. Schlotterbeck, A. Grossmann, and C. Zimmermann, *Phys. Rev. Lett.* **87**, 230401 (2001).
8. D. S. Petrov, G. V. Shlyapnikov, and J. T. M. Walraven, *Phys. Rev. Lett.* **85**, 3745 (2000).
9. D. S. Petrov, G. V. Shlyapnikov, and J. T. M. Walraven, *Phys. Rev. Lett.* **87**, 050404 (2001).
10. F. Dalfovo, S. Giorgini, L. P. Pitaevskii, and S. Stringari, *Rev. Mod. Phys.* **71**, 463 (1999).
11. S. Dettmer, D. Hellweg, P. Ryytty, J. J. Arlt, W. Ertmer, K. Sengstock, D. S. Petrov, G. V. Shlyapnikov, H. Kreutzmann, L. Santos, and M. Lewenstein, *Phys. Rev. Lett.* **87**, 160406 (2001).
12. D. Hellweg, S. Dettmer, P. Ryytty, J. J. Arlt, W. Ertmer, K. Sengstock, D. S. Petrov, G. V. Shlyapnikov, H. Kreutzmann, L. Santos, and M. Lewenstein *Appl. Phys. B* **73**, 781 (2001).
13. J. J. García-Ripoll, V. Pérez-García and P. Torres, *Phys. Rev. Lett.* **83**, 1715 (1999); J. J. G. Ripoll and V. M. Pérez-García, *Phys. Rev. A* **59**, 2220 (1999).
14. P. G. Kevrekidis, A. R. Bishop, and K. Ø. Rasmussen, *J. Low Temp. Phys.* **120**, 205 (2000).
15. K. Staliunas, S. Longhi, G. J. de Valcarcel, *cond-mat/0204517*.
16. D. S. Jin, J. R. Ensher, M. R. Matthews, C. E. Wieman, and E. A. Cornell, *Phys. Rev. Lett.* **77**, 420 (1996); M.-O. Mewes, M. R. Andrews, N. J. van Druten, D. M. Kurn, D. S. Durfee, C. G. Townsend, and W. Ketterle, *Phys. Rev. Lett.* **77**, 988 (1996).
17. D. S. Petrov, M. Holzmann, and G. V. Shlyapnikov, *Phys. Rev. Lett.* **84**, 2551 (2000).
18. V. N. Popov, *Functional Integrals in Quantum Field Theory and Statistical Physics*, (D. Reidel Pub., Dordrecht, 1983).
19. S. I. Shevchenko, *Sov. J. Low Temp. Phys.* **18**, 223 (1992).
20. S. Stringari, *Phys. Rev. A* **58**, 2385 (1998).
21. Yu. Kagan, E. L. Surkov, and G. V. Shlyapnikov, *Phys. Rev. A* **54**, R1753 (1996).
22. Y. Castin and R. Dum, *Phys. Rev. Lett.* **77**, 5315 (1996).
23. Note that Eq. (8) was misprinted in [12] and that the correct equation is given here.
24. M.-O. Mewes, M. R. Andrews, N. J. van Druten, D. M. Kurn, D. S. Durfee, and W. Ketterle, *Phys. Rev. Lett.* **77**, 416 (1996).
25. W. Ketterle and H.-J. Miesner, *Phys. Rev. A* **56**, 3291 (1997).

- 26. M. J. Holland, D. S. Jin, M. L. Chiofalo, and J. Cooper, Phys. Rev. Lett. **78**, 3801 (1997).
- 27. M. Cartmell, *Introduction to linear, parametric and non-linear vibrations*, (Chapman and Hall, 1990); L. D. Landau and E. M. Lifshitz, *Course of theoretical physics* Vol. 1, (Pergamon Press, 1969).
- 28. W. Ketterle, and N. J. van Druten, Phys. Rev. A **54**, 656 (1996).
- 29. T. L. Ho, and M. Ma, J. Low Temp. Phys. **115**, 61 (1999).
- 30. P. A. Ruprecht, M. Edwards, K. Burnett, and C. W. Clark, Phys. Rev. A **54**, 4178 (1996); M. Brewczyk, K. Rzażewski, and C. W. Clark, Phys. Rev. A **75**, 488 (1998).